Exploring the potential of MSC secretome to counteract APAP-induced hepatic injury *in vitro*

Ribeiro, D.[1,2], Rodrigues, J. S.[2], Camões, S.P.[2], Serras, A. S.[2], Branco, S.[1,2], Miranda, J. P.[2]

[1] Instituto Superior Técnico, Universidade de Lisboa, Av. Rovisco Pais, Nº1, 1049-001 Lisboa, Portugal.
[2] Research Institute for Medicine (iMed.ULisboa), Faculty of Pharmacy, Universidade de Lisboa, Av. Prof. Gama Pinto, 1649-003 Lisboa, Portugal.

Abstract

Acetaminophen (APAP)-induced hepatotoxicity is the major cause of drug-induced liver injury (DILI), accounting for 40-70 % of acute liver failure in the United Kingdom and Europe. Current therapies do not meet the global need or display a narrow therapeutical window. Thus, mesenchymal stem cells (MSCs) and their paracrine factors emerge as alternative therapeutical approaches to enhance liver regeneration.

Emerging evidence sustains that MSC fate and behaviour is altered in response to the microenvironmental niche *in vitro* and *in vivo*. Thus, priming MSCs with medium from hepatic injured cells (SOS medium) was attempted to produce an MSC-secretome more targeted for liver injury. Herein, medium from an APAP-induced hepatic injury *in vitro* model (SOS medium) was produced by incubating HLCs (human hepatocyte-like cells derived from stem cells) with the estimated APAP IC50 value (30 mM) for 8 hours. Upon APAP incubation, it could be observed that HLCs altered their morphology, expressing APAP-induced hepatotoxicity genes related with endoplasmic reticulum stress and apoptosis. Additionally, the APAP-induced liver injury model was characterized in 3D cultures, seeming to suggest a higher hepatoprotective effect than in 2D cultures.

Afterwards, MSCs were primed with the SOS medium (5x concentrated), modulating their secretome into a more angiogenic phenotype, up-regulating *SDF-1* and *TNF-A*. Importantly, upon exposure to MSCs-primed secretome, APAP-injured HLCs displayed pro-regenerative effects, up-regulating *CCND1*, *C-MET*, *VEGF-A* and *FGF-2*. Results also showed increased cell proliferation in HLCs exposed to 5 and 15 mM APAP for 24 hours incubated with the MSCs-primed secretome. Indeed, the priming strategy displayed therapeutic relevance in 15 mM APAP injured HLCs.

In sum, the APAP-induced liver injury *in vitro* model mimicked the injury microenvironment and increased the MSC secretome potential for enhanced hepatic regeneration.

Keywords: hepatocyte-like cells; APAP; Drug-induced liver injury; secretome; mesenchymal stem cells; liver regeneration.

1. Introduction

The strategic anatomic position of the liver close to the gastrointestinal tract, the structural organization of the liver sinusoidal space and the blood supply from the portal vein makes the liver an organ highly exposed to xenobiotics. The xenobiotics biotransformation within hepatocytes generates reactive metabolites that interfere with specific cell functions. After exposure to toxic doses of drugs or viral infections, acute liver failure (ALF) caused by a sudden decompensation of the hepatic function, triggers inflammatory or fibrotic responses. Indeed, drug-induced liver injury (DILI) is responsible for 13 % of cases ALF, being acetaminophen (APAP)-induced hepatotoxicity the major cause.[1] APAP is a highly used anti-pyretic and analgesic drug, responsible for 46 % of all ALF cases in the United States and between 40 to 70 % of all cases in the United Kingdom and Europe.[2]

APAP is metabolized by phase I and II enzymes of the liver's drug metabolism within hepatocytes. Through sulfation, glucuronidation and oxidation APAP is converted into APAP sulfate form (APAP-sulfate), APAP glucuronide form (APAP-gluc) and into *N*-acetyl-*p*-benzoquinone imine (NAPQI), respectively. The latter is a reactive metabolite detoxified by intracellular glutathione (GSH) and excreted as nontoxic conjugates of cysteine and mercapturic acid (APAP-cys). Under excessive doses of APAP, sulfation and glucuronidation pathways become saturated and higher amounts of APAP are oxidated into NAPQI by the cytochrome P450 (CYP450) enzymes, depleting GSH stores.[3] Then, NAPQI covalently binds to cysteine groups on cellular proteins, especially mitochondrial proteins, modifying intracellular structures and forming NAPQI-adducts. This step is irreversible and results in dysfunctions on mitochondrial respiration, generating free radicals, namely, superoxide. Thus, mitochondrial anti-oxidant defences are compromised leading to an initial mitochondrial oxidative stress and oxidation of mitochondrial proteins such as thioredoxin (Trx). Trx detaches from apoptosis signal-regulating kinase 1 (ASK1) which becomes activated in the cytosol. During APAP hepatotoxicity, mixed-lineage kinase 3 (MLK3) is also activated upon oxidative stress. The counterplay between activated ASK1 and MLK3 phosphorylates mitogen-activated protein kinase kinase 4 (MKK4) which subsequently phosphorylates c-jun N-terminal kinase (JNK) in the cytosol. The phosphorylated JNK inhibits mitochondrial electron transport in the mitochondria, increasing its oxidative stress. Additionally, Bcl-2-associated X protein (Bax) translocation from the cytosol to the mitochondria enhances oxidative stress and the release of mitochondrial intermembrane proteins, which move to the nucleus and promote DNA fragmentation. The last event induces the activation of receptor-interacting protein kinases (RIPK) 3/1 resulting in hepatocyte necrosis.[4,5] NAPQI also covalently binds to endoplasmic reticulum (ER) proteins, causing ER stress and the dissociation of chaperone binding immunoglobulin protein, which activates the three ER stress sensors – inositol-requiring enzyme 1 alpha (IRE1α), double-stranded RNA-dependent protein kinase-like ER kinase (PERK) and activating transcription factor (ATF)-6 – inducing the transcription of X-box binding protein 1 spliced (XBP1), ATF-4 and active N-terminus cytosolic fragment (ATF-6N), respectively. These proteins translocate to the nucleus and regulates the expression of ER stress target genes, such as C/EBP homologous protein (CHOP), with a pro-damage role in liver injury by inhibiting liver regeneration.[6,7]

The liver has the unique ability to intrinsically regenerate until a certain extension of damage, resorting, mostly, to hepatocytes. The liver regeneration process is divided in three phases: priming, progression and termination. The priming phase is the first phase of the liver regeneration and promotes the activation of numerous genes within few minutes after injury. Therefore, quiescent hepatocytes convert from G0 to G1 of the cell cycle due to pro-inflammatory cytokines, namely, tumour necrosis factor alpha (TNF-α) and interleukin (IL)-6, released by Kupffer cells, which through the nuclear factor kappa light chain enhancer of activated B cells (NF-kB), JNK, Janus

kinase-signal transducer and activator of transcription 3 (STAT3), extracellular signal-regulated protein kinase (ERK) 1/2 signally pathways, respectively, induce the transcription of several proliferative genes, including cyclin D1.[8,9,10]

The second phase is termed progression, in which growth factor receptors are activated and hepatocytes progress from the G1 phase to the mitosis, promoting proliferation. Additional signalling factors named mitogens secreted by different cell types assist this replicative cycle and can be classified as complete or auxiliary. Complete mitogens, namely, hepatocyte growth factor (HGF) and epidermal growth factor receptor (EGFR) ligands act like paracrine factors inducing hepatocyte proliferation and DNA synthesis through the Ras-Raf-mitogen-activated protein kinase (MAPK) signalling and the phosphatidylinositol 3-kinase (PI3K)/ protein kinase B (AKT) signalling pathway. Notably, the loss of either EGFR or c-Met, which is the HGF cell surface receptor in hepatocytes and cholangiocytes, delays liver repair and the regeneration process is completely blocked by the loss of both receptors. HGF in healthy liver is bound to the extracellular matrix (ECM) of endothelial and Kupffer cells, but after injury it is released to the bloodstream and additional HGF is produced by hepatic stellate cells (HSCs) and endothelial cells. This additional HGF production is detected by c-Met, which induces cyclin and cyclin-dependent kinases (CDKs) activation, responsible for cell cycle regulation and the initiation of DNA synthesis. Regarding the EGFR ligands, heparin-binding (HB)-EGF is produced by Kupffer and endothelial cells in the liver, EGF is secreted by Brunner's gland in the duodenum and transforming growth factor (TGF)-α is secreted by hepatocytes. In turn, auxiliary mitogens, such as bile acids, norepinephrine, insulin, TNF-α, IL-6, estrogen and serotonin, promote and accelerate the proliferation step cell cycle entry by boosting the effect of direct mitogens.[8,9,11] Another mechanism behind liver regeneration during the priming and proliferation stage is angiogenesis. The cross-talk between liver sinusoidal endothelial cells, HSCs and hepatocytes induces the formation of new microvasculature from pre-existing blood vessels and mature endothelial cells. In a hypoxia-stimulated environment, hypoxia-induced factors (HIFs) react to reduced oxygen levels by up-regulating vascular endothelial growth factor (VEGF), VEGF receptors, endothelial nitric oxide synthase, vascular endothelial cadherins, platelet endothelial cell adhesion molecule-1, matrix metalloproteinases, angiopoietins, integrins, etc. These factors mediate vasodilation, increase vascular permeability and endothelial cell membrane remodelling, allowing for endothelial cell migration, proliferation and organization of new vessels.[12]

Lastly, termination is the last step and is related to the cessation of proliferation through the activation of key factors. For example the TGF-β, released by hepatocytes, stellate, endothelial and Kupffer cells is a pro-inhibitory cytokine that inhibits hepatocyte proliferation by blocking the function or production of CDKs and cyclins. Similarly, activin A produced by hepatocytes also hinders hepatocyte proliferation.[8,9] Moreover, the hepatocyte nuclear factor (HNF)4-α, which is a transcription factor essential for the maintenance of the hepatic functions, plays a key role in the hepatocytes exit from the cell cycle, aiding the termination of the liver regeneration.[13]

Upon great disruption of the hepatic parenchyma, the liver is unable to replace the dying hepatocytes, progressing to a liver failure status. *N*-acetylcysteine (NAC) is an effective antidote to APAP hepatotoxicity but its administration must occur within 8 hours of the overdosage. Hence, in some situations liver transplantation is the only viable option, being the second most common solid organ transplantation, yet the current rate of transplantation only meets 10 % of the global need.[14] Therefore, there is the need to thoroughly understand the underlying mechanisms of liver injury and regeneration to develop more efficient alternative therapies.

Recently, stem cells therapeutics have arisen, since they do not rely on the availability of organ donors and have the ability to self-renew maintaining its undifferentiated state and to differentiate into distinct cell types. Particularly, mesenchymal stem cells (MSCs) offer important advantages for their therapeutic application in tissue repair and regeneration since they are easy to obtain, maintain, expand and cryopreserve, without losing their viability, genome stability neither their replicative capacity, with the plus of being free from ethical concerns.[15] Even though MSCs have the capacity to differentiate into hepatocyte-like cells (HLCs), MSC cell-based therapies present some issues, namely, the lack of a standardized protocol for isolation and for *ex vivo* expansion, the decline in the engraftment and homing ability, the poor survival rate, the impaired differentiation ability of transplanted MSCs *in vivo* as well as the risks associated with the transplantation of undifferentiated and proliferative cells. Thus, rather than differentiating into liver cells the therapeutic benefit of MSCs in regenerative medicine may be related with cell-free therapies, overcoming the cell culture issues.[16] Indeed, recent data revealed that MSCs alleviate liver failure mainly through trophic and immunomodulatory factors. These factors induce pro-healing mechanisms after acute damage, altering the tissue microenvironment; support hepatocyte function, promote the proliferation of residual hepatocytes, inhibit hepatocyte apoptosis, reverse liver fibrosis and promote angiogenesis.[17] The paracrine factors secreted by MSCs have the capacity to immunomodulate the response of the immune system while having several effects: anti-inflammatory, anti-fibrotic, anti-apoptotic and angiogenic.[18,19] The *in vitro* cultured MSCs secrete cytokines, chemokines, growth factors and immunomodulatory molecules into their culture medium, composing the MSC secretome or conditioned medium (CM). Moreover, MSCs have toll-like receptors which allow them to sense their microenvironment and act accordingly to it, polarizing into a pro-inflammatory or an immunosuppressive phenotype.[20] Therefore, pre-conditioning, commonly designated as priming, of the culture microenvironment with hypoxia[21] or small molecules[22,23], three-dimensional (3D) culture systems[24,25] or genetic manipulations[26,27] have been performed to enhance the clinical outcome of MSCs and their secretion of paracrine factors into the culture medium.

Accordingly, this work hypothesised that the modulation of the MSCs secretome with inflammatory signals from injured liver, mimicking the liver injury environments, would enhance the hepatic regenerative capacity. As such the objectives of this work were: to analyse the mechanisms related with APAP-induced hepatotoxicity, to prime MSC-mediated paracrine mechanisms by incubating MSCs with media collected from APAP-induced liver injury in *in vitro* cultures (SOS medium) and to evaluate the therapeutical effect of the primed-MSC secretome in an MSC-derived HLC *in vitro* model of APAP-induced injury.

2. Materials and Methods

Reagents

Trypsin-EDTA, fetal bovine serum (FBS), insulin-transferrin-selenium (ITS) and penicillin streptomycin were purchased from Gibco®/Thermo Fisher Scientific®. HGF, fibroblast growth factor (FGF)-2 and FGF-4, oncostatin M (OSM), dexamethasone and 5-azacytidine (5-AZA) were purchased from Peprotech®. Amphotericin B

was purchased from Biochrom® and bovine serum albumin (BSA) from PanReac®. Lastly, Iscove's modified Dulbecco's medium (IMDM), minimum essential medium eagle alpha modification (α-MEM), EGF, dimethyl sulfoxide (DMSO), nicotinamide, trypan blue and 4-acetamidophenol were acquired from Sigma-Aldrich®.

Cell culture

hnUCM-MSCs were isolated according to Miranda *et al*. (2015)[28] and Santos *et al.* (2015)[29]. In two-dimensional (2D) culture, hnUCM-MSCs were expanded as undifferentiated cells in a growing medium consisting in α-MEM with 10 % (v/v) FBS, incubated at 37 °C in 5 % carbon dioxide (CO2) humidified atmosphere. Cell passage was performed with 0.05 % Trypsin-EDTA incubation for 5 minutes every 2 - 3 days when cell confluence reached 70 - 80 %. Cells were counted under an Olympus CK30-F200 (Olympus Optical®) inverted microscope and cell viability was assessed through trypan blue exclusion method. Cell culture photographs were acquired using a Moticam 2500 5.0M Pixel (Motic®) camera mounted on Olympus CK30-F200 inverted microscope and images were collected using Motic Images Plus 3.0 software (Motic®).

Collagen coating

Following the protocol described in Rajan et al. (2006)[30], rat-tail collagen was produced in house for culture flasks and well plates coating. The extracted rat-tail collagen was dissolved in 0.1 % (v/v) acetic acid achieving a stock solution concentration of 1 mg/mL. The stock solution was diluted to 0.2 mg/mL in a volume of phosphate buffered saline (PBS) which assured total culture surface coverage. The collagen polymerization occurred after 1-hour incubation at 37 °C. Afterwards, the cell culture surfaces were washed with PBS before cell inoculation.

Hepatocyte differentiation protocol

The hepatocyte differentiation protocol herein followed is described in Cipriano *et al*. (2017)[31],[32]. hnUCM-MSCs were seeded in culture flasks pre-coated with rat-tail collagen at a density of 1.5 x 10^4 cells/cm^2, reaching a cell confluency of 90 % within 24 hours after inoculation. A three-step differentiation protocol was performed to generate HLCs using as basal medium (BM) IMDM with 1 % (v/v) penicillin-streptomycin-amphotericin B. In the first step the cells were incubated for 48 hours in BM supplemented with 2 % (v/v) FBS, 10 ng/mL of EGF and 4 ng/mL of FGF-2, for endoderm commitment and foregut induction. In the second step, hepatoblasts and liver bud formation was induced by maintaining the cells for 10 days in BM supplemented with 4 ng/mL of FGF-2, 10 ng/mL of FGF-4, 20 ng/mL of HGF, 0.61 g/L of nicotinamide and 1 % (v/v) ITS. At day 10 of differentiation (D10), 1 % (v/v) DMSO was added to the medium. Lastly, in the third step, for hepatoblast differentiation and hepatocyte maturation, cells were maintained in BM supplemented with 8 ng/mL of OSM, 1 µM of dexamethasone, 1 % (v/v) DMSO and 1 % (v/v) ITS from D13 onwards, defined as differentiation medium (DM). At D17, cells were trypsinized with 0.25 % Trypsin-EDTA solution for 3 minutes and re-inoculated in DM containing 20 µM of 5-AZA and 5 % (v/v) FBS into (1) 2D pre-coated culture flasks for the production of SOS medium, 96-well plates for cell viability assays, 6-well plates for quantitative real-time polymerase chain reaction (qRT-PCR) analysis at a density of 2 x 10^4 cells/cm^2; and (2) ultra-low attachment plates and flasks for 3D spheroid culture at 5.0 x 10^5 cells/mL. 24 hours after the inoculation, the medium was changed to remove 5-AZA and FBS. Cells were maintained in DM up to D27 of culture with medium replacement every 3 - 4 days.

Conditioned medium production

SOS medium

At D27, HLCs in 2D culture flasks were incubated with 30 mM APAP. After 8-hour exposure, cells were washed two times with PBS and the medium was replaced by fresh DM without APAP, at a final volume of 25 mL per 175 cm^2 t-flask or 10.7 mL per 75 cm^2 t-flask. After 24h, the SOS medium was collected under sterile conditions and centrifuged firstly at 300x*g*, 25 ºC, for 10 minutes, and then at 2700x*g*, 4 ºC for 30 minutes. The injured HLCs were harvested for total protein quantification and qRT-PCR analysis. The same procedure was applied to 3D-cultured HLCs, exposing them for 8 hours to 30 mM APAP at D27 and recovering the cells 24 hours later. Also, samples from 2D-cultured HLCs exposed to 30 mM APAP for 24 hours at D27 were collected for qRT-PCR analysis. The SOS medium was concentrated in Amicon® Ultra-15 (Millipore®) 3 kDa cut-off centrifugal concentrators as per manufacture's recommendations. Samples were stored at -80 ºC until further use.

Pre-conditioning of hnUCM-MSCs: production of conditioned medium (MSC-CM)

For the production of MSC-CM, hnUCM-MSCs, with a maximum of 15 passages, were inoculated at a density of 1.0x10^4 cells/cm^2 in 175 cm^2 and 75 cm^2 t-flask with α-MEM and 5 % (v/v) FBS. When 60 % confluence was reached, cells were washed with PBS and α-MEM. For priming MSC-CM with the SOS medium, hnUCM-MSCs medium was replaced by α-MEM without FBS (90 % of the final volume) and with 10 % of SOS medium 50x concentrated, at a final volume of 18 mL per 175 cm^2 t-flask and 8 mL per 75 cm^2 t-flask. After 24 hour-priming, the cells were washed with PBS and α-MEM and the medium was replaced by fresh α-MEM without FBS, at a final volume of 25 mL per 175 cm^2 t-flask and 10.7 mL per 75 cm^2 t-flask. After conditioning for 48 hours, primed MSC-CM (pMSC-CM) was collected under sterile conditions and centrifuged as mentioned previously. Control MSC-CM (cMSC-CM) was produced from a 3-day incubation of hnUCM-MSCs with α-MEM and 5 % (v/v) FBS, followed by 48 hours with α-MEM without FBS at a final volume of 25 mL per 175 cm^2 t-flask and 10.7 mL per 75 cm^2 t-flask. Cells were harvested for total protein quantification and qRT-PCR analysis. As described previously, CM was concentrated and stored at -80 ºC until further use.

Cell viability assays

APAP cytotoxicity and the effect of CM in HLCs upon APAP exposure were evaluated using the MTS reduction assay (Promega®). Cell viability was measured, according to the manufacturer's instructions. For evaluating APAP cytotoxicity, HLCs at D27 seeded in 96-well plates, were exposed to 0, 5, 10, 15, 20, 30, 50 and 60 mM APAP for 24 hours. The estimated half-maximal inhibitory concentration (IC_{50}) was calculated through a non-linear regression fit.

For assessing the effect of CM in HLCs viability upon APAP exposure, HLCs were exposed to 0, 5, 15 and 30 mM APAP at D27. After a 24-hour exposure, cells were washed with PBS and the medium was replaced by DM with 10 % (v/v) of pMSC-CM or cMSC-CM 100x concentrated for other 24 hours. 10 % (v/v) DMSO was used as negative control and IMDM as positive control. Results were presented as relative percentages to the positive control, which was considered as 100 % of cellular viability. The absorbance was measured at 490 and 690 nm using microplate reader SPECTROstar Omega (BMG Labtech®).

Gene expression

Total RNA was isolated from samples with 0.5-1.0 x 10^6 cells using Trizol® (Life Technologies®) and extracted according to the manufacturer's instructions. RNA concentration was

determined by measuring absorbance at 260 nM in LVis Plate mode (SPECTROstar Omega, BMG Labtech®). The 260/280 nm ratio was used as purity measurement for protein presence, considering ratios between 1.8-2.0. c-DNA was synthesized from 1 µg of RNA using NZY First Strand cDNA Synthesis Kit (NZYTech®), following the manufacturer instructions. qRT-PCR was performed using PowerUp™ SYBR® Green Master Mix (Life Technologies®). Master mix was prepared for a final reaction volume of 15 µL, using 2 µL of template cDNA and 0.333 µM of forward and reverse primers (Annexes, table A). The reaction was performed on QuantStudio™ 7 Flex Real-Time PCR System (Applied Biosystems®) consisting of an activation step of Uracil-DNA Glycosylase (UDG) at 50 °C for 2min, a denaturation step at 95 °C for 10 minutes, followed by 40 cycles of denaturation at 95 °C for 15 seconds and annealing and extension at 60 °C for 1 minute. As a quality and specificity measure, a dissociation stage which determines the melting temperature of a single nucleic acid target sequence was added. Blank controls with no cDNA templates were performed to rule out contamination. The comparative Ct method ($2^{-\Delta\Delta Ct}$) was used to quantify gene expression, which was normalized to the reference gene (β-actin).

Protein quantification

For total protein quantification, cells were lysed with 0.1 M sodium hydroxide (NaOH) overnight at 37 °C. Protein concentration was determined through the calorimetric Bradford assay with protein assay dye reagent concentrate (Bio-rad®) diluted in 1:5 in Milli-Q® water. The absorbance was measured at 595 nm using microplate mode on SPECTROstar Omega.

Statistical analysis

Statistical data analysis was performed using GraphPad Prism version 9.0 (GraphPad Software®). The results are shown as the average ± SD. Data comparisons were analysed by two-way ANOVA with Šidák's test and differences were statistically significant for $p < 0.05$.

3. Results and discussion

APAP toxicity in hepatocyte-like cells (HLCs)

Over the years, animal models have been used to study liver mechanisms, mimic liver diseases and assess novel therapeutics, enabling the study of whole organs and living organisms. However, the inherent interspecies differences, the ethical concerns and the impossibility to evaluate molecular mechanisms urged the need for more reliable hepatic models which predicted human toxic events, minimizing the amount of drug failures.[33] Alternatively, primary human hepatocytes (PHH) resembled the specific metabolism and functionality of the human liver, but their scarcity and suitability only for short-term studies in monolayer cultures due to their rapid loss of functionality hindered their application.[34] Hence, researchers explored hepatocyte immortalized cell lines (e.g. HepG2 and HepaRG) derived from hepatomas or through genetic manipulations. However, these cell lines presented altered metabolic functions and genetic abnormalities, failing to mimic human physiology. Therefore, *in vitro* stem cell-differentiation into HLCs arose, overcoming the limitations related with the aforementioned cell sources.[35]

HLCs can be differentiated from ESCs, iPSCs and MSCs, but MSCs characteristics and benefits were optimal for *in vitro* models. Indeed, MSC-derived HLCs presented hepatocyte-specific gene expression and functions, namely, urea and glycogen production.[36] Among the different MSCs sources, hnUCM-MSCs were more favourable to differentiate into HLCs for a human-based *in vitro* liver model, owing to the lack of major ethical issues, the low risk of viral transmission, the low immunogenicity, the abundant and non-invasive availability and to its more primitive origin.[37]

The three-step protocol herein followed for hepatocyte differentiation using hnUCM-MSCs was adapted from the previously described and characterized in Cipriano *et al.* (2017).[31,32] From D21 onwards HLCs were metabolically competent, displaying drug transporter and phase I and II enzymes expression and activity.[31,38] Therefore, the herein presented results were performed at D27 of the differentiation protocol.

To assess the effect of APAP in HLCs, we plotted the APAP dose-response curve in HLCs at D27 through the MTS cell viability assay (Figure 1). The cells were exposed to 5, 10, 15, 20, 30, 50 and 60 mM of APAP for 24 hours.

From the resulting dose-response curve, the IC_{50} was determined as 29.64 ± 0.85 mM APAP for a 24-hour exposure in HLCs. Hereafter, we approximated the APAP IC_{50} value to 30 mM. Therefore, as a starting point, we considered the IC_{50} value for the APAP-induced liver injury in *in vitro* cultures, namely, for the SOS medium production, since it was a reasonable and sufficient APAP concentration to induce hepatotoxicity while maintaining cells functional.

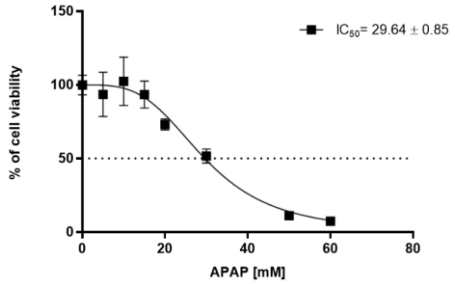

Figure 1 - APAP toxicity in HLCs. The HLCs were incubated with 5, 10, 15, 20, 30, 50 and 60 mM of APAP for 24 hours (n=2). The percentage of live cells is calculated relatively to non-treated HLCs at D28.

APAP-induced liver injury in 2D and 3D HLC *in vitro* cultures reveal differential liver injury-related gene expression levels

APAP induced morphological changes and altered gene expression in 2D-cultured HLCs

Upon APAP-induced injury human hepatocytes are known to secrete specific cytokines. Indeed, CM from APAP-exposed human ESC-derived HLCs revealed an increase in inflammatory cytokines and activated immune cells, triggering an immune-mediated hepatotoxicity.[39] Herein, to produce the APAP-induced HLCs injury medium with inflammatory signals (SOS medium), which we hypothesised that could modulate the MSC secretome, we exposed HLCs to 30 mM APAP. Ongoing work in our laboratory group, determined through total protein quantification of HLCs exposed to APAP (data not shown) that the level of cell injury was similar either at 24-hour (the incubation time used for the dose-response curve) or at 8-hour exposure to APAP. Therefore, to ensure minimal loss of injury signals and the presence of the initially produced inflammatory cytokines, we established an 8-hour APAP exposure for the SOS medium production. After 8-hour APAP exposure, the medium was replaced by fresh medium to remove the presence of APAP. After 24h conditioning period, the conditioned medium was collected (SOS medium), in order to guarantee that HLCs' inflammatory signals consequent of the APAP toxicity were present.

Throughout the differentiation protocol, the hnUCM-MSC-derived HLCs showed significant differences in morphology as a result of the sequential exposure to cytokines, growth factors and small molecules which mimicked the liver embryonic development, transitioning from a fibroblast-like to an epithelial polygonal shape

morphology with binucleated cells, seen in Figure 2 a). The HLCs morphology resultant from an 8-hour exposure to 30 mM APAP at D27 is presented in Figure 2 b). Upon APAP exposure, HLCs modified their hepatocellular morphology and the detachment of some cells from the culture flask was visible as a result to the deleterious drug. Their morphology 24 hours after removing APAP, at the end of the conditioning period (Figure 2 c)), exhibited a significant improvement, re-gaining their polygonal shape, suggesting that HLCs had the capacity to recover until a certain extent after the drug removal.

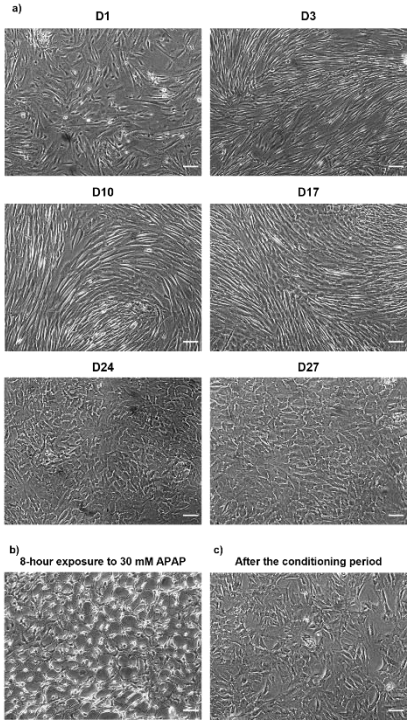

Figure 2 - APAP altered HLCs' polygonal shape morphology and caused detachment. a) morphological changes in 2D-cultured HLCs throughout the differentiation protocol, from D1 to D27; b) HLCs' morphology after an 8-hour exposure to 30 mM APAP; b) HLCs' morphology at the end of the conditioning time to produce the SOS medium. HLCs were exposed to APAP at D27. After APAP exposure, the medium was replaced by fresh medium without APAP. Scale bar = 100 µm.

Under excessive doses of APAP, the APAP reactive metabolite NAPQI accumulates in the liver, leading to the formation of NAPQI-adducts, causing mitochondrial oxidative stress, ER stress, DNA fragmentation and hepatocyte necrosis. Therefore, to evaluate the effect of APAP in HLCs we assessed the expression level of *ASK1*, *RIPK3*, *ATF-6* and *BAX*, involved in the APAP-induced hepatotoxicity, namely, mitochondrial oxidative stress, necroptosis, ER stress and apoptosis, respectively. Additionally, expression levels of *HNF4-A* and *TNF-A* were also analysed. The interest in the transcription factor HNF4-α relied on its crucial role in hepatocyte differentiation during embryogenesis, in the maintenance of the hepatic function, in the regulation of the hepatic epithelial morphology and in the enhancement of MSC differentiation. In decompensated livers, in animal models of chronic liver failure and in HCC, the nuclear *HNF4-A* revealed to be significantly down-regulated.[40,41,42] Moreover, this transcription factor had a crucial role in the termination phase of liver regeneration, since its re-expression after initial decrease was pivotal for hepatocytes exit from the cell cycle.[13] In regard to TNF-α, this pleiotropic cytokine influenced cell growth, differentiation and metabolism, being involved in both systemic inflammation and regeneration. Indeed, *TNF-A*, one of the most abundant early mediators in injured tissue, showed up-regulation during liver injury.[43,44] Moreover, TNF-α also prime the hepatic liver regeneration cycle.

Therefore, a panel of genes involved in APAP-induced toxicity were quantified in order to shed light on the effects of APAP exposure to the cells. The gene expression profile of HLCs was evaluated at the time of the SOS medium collection, i.e., in HLCs exposed for 8 hours to 30 mM APAP followed by a 24-hour conditioning with fresh medium without APAP. Results are shown in Figure 3, relative to non-injured HLCs recovered at D28.

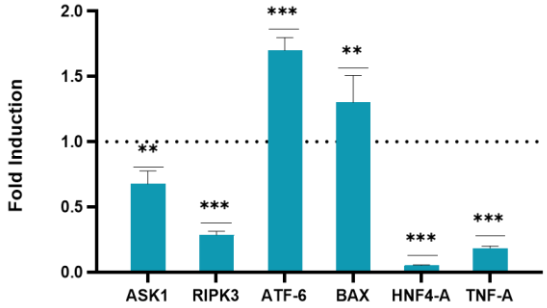

Figure 3 - Endoplasmic reticulum stress and apoptosis were induced in HLCs following APAP exposure. Gene expression of HLCs with an 8-hour exposure to 30 mM APAP, at D27, followed by a 24-hour conditioning with fresh medium without APAP, relative to non-injured HLCs recovered at D28. Data represented as average ± SD (n=1-3). **, *** significantly differed from the non-injured HLCs gene expression with $p < 0.01$ and $p < 0.001$, respectively.

The results presented in Figure 3 showed that only *ATF-6* ($p < 0.001$) and *BAX* ($p < 0.01$) were significantly overexpressed relatively to non-injured cells, suggesting APAP-induced hepatotoxicity through ER stress and apoptosis. Concordantly with the literature, *HNF4-α* was dramatically reduced ($p < 0.001$), relatively to control, indicating the existence of hepatic injury.[40,41,42]

Since *ASK-1* represents the mitochondrial oxidative stress induced by NAPQI, its inhibition ($p < 0.01$) relatively to non-injured HLCs, might be related with the wash-out of APAP and, consequently, its reactive metabolite NAPQI, during the replacement of medium for the conditioning period. The stress-induced environment triggered by APAP exposure might have stimulated HLCs to intrinsically regenerate and regain their normal phenotype during the following 24-hour conditioning period, seen with the inhibition of *ASK1* and *RIPK3* and the morphological recovery in Figure 2 c).

The overall presented results seemed to suggest that upon an 8-hour exposure to 30 mM APAP, HLCs suffered damage and activated APAP-related hepatotoxicity pathways, implying that the APAP-induced liver injury *in vitro* culture might have mimicked, to a certain degree, the liver injury microenvironment. Therefore, the SOS medium might display the capacity to prime/modulate the hnUCM-MSCs into a regenerative status.

Even though the *in vitro* APAP-induced liver injury through 2D culturing of HLCs seemed to replicate liver injury, several strategies have been studied to identify and further optimize *in vitro* conditions for hepatocyte maturation, assessment of drug toxicities and disease mechanisms, namely, 3D cell culturing.

3D culturing of HLCs to establish an in vitro APAP-induced liver injury model

The advantages of 3D-cultured HLCs rely on a high cell-to-cell and cell-to-ECM contact, on a nutrient and oxygen gradients and on cell polarization which are essential for liver development.[45] 3D aggregates surge from the adherence of cells to one another, forming a spherical aggregate. Regarding hepatogenic differentiation, 3D culturing of hESCs-derived and iPSCs-derived HLCs improved hepatocyte phenotype, namely, the

biotransformation activity.[46,47] Likewise, the MSC differentiation into HLCs in 3D cultures showed higher liver functional features, namely, phase I and II metabolization capacity and urea and albumin production.[32] Therefore, taking a step forward in this work, we started the development of an APAP-induced liver injury model in 3D culture. As such, from D17 onwards HLCs were cultured in ultra-low attachment culture plates. The inoculated cells formed clusters which progressively aggregated into small spheroids, as seen in Figure 4 a). At D27, 3D-cultured HLCs were exposed to 30 mM APAP for 8 hours (Figure 4 b)), as in 2D cultures. Afterwards, the medium was replaced to remove APAP and followed by the 24-hour conditioning period (Figure 4 c)), for the production of the SOS medium in 3D culture.

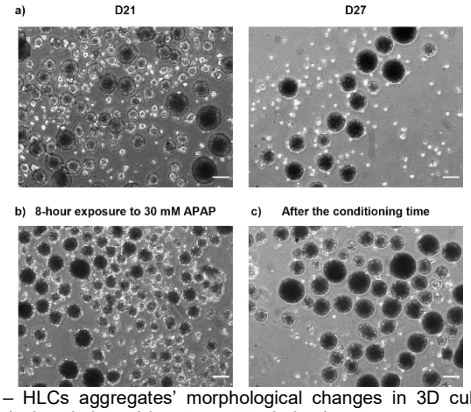

Figure 4 – HLCs aggregates' morphological changes in 3D culturing. a) morphological variation of hnUCM-MSC-derived HLCs aggregates at D21 and D27 cultured in ultra-low attachment plates; b) HLCs aggregates' morphology after an 8-hour exposure to 30 mM APAP; c) HLCs aggregates' morphology at the end of the conditioning time. HLCs aggregates were exposed to APAP at D27. Scale bar = 100 µm.

The HLCs aggregates' diameters in different days of the differentiation protocol, upon an 8-hour exposure to 30 mM APAP (at D27) and at the end of the conditioning time (at D28) are presented in Figure 5.

Figure 4 illustrates the HLCs aggregates' increased cell density from D21 to D27 which was reflected on the augmentation of their diameter (Figure 5). After an 8-hour exposure to 30 mM APAP (Figure 4 b)), the spheroids showed an irregular border and the number of dead cells in suspension increased, resulting in a slight reduction of their diameter. Alike 2D-cultured HLCs (Figure 2 c)), the aggregates showed improvements in their morphology and diameter size after removing the deleterious drug (Figure 4 c)).

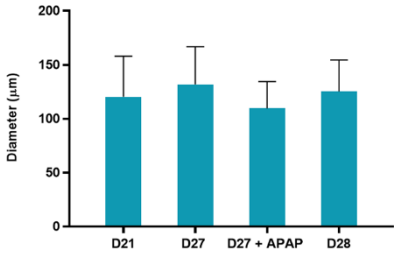

Figure 5 – HLCs aggregates reduced their diameter upon APAP exposure. HLCs aggregates' diameters, in µm, at D21, D27, after an 8-hour exposure to 30 mM APAP at D27 (D27 + APAP) and at D28 at the end of the conditioning period. The diameters were measured through phase contrast microscopy images of HLCs inoculated in ultra-low attachment culture plates.

Afterwards, to evaluate if APAP exposure affects differently 2D and 3D-cultured HLCs, a panel of APAP-related hepatotoxicity genes was assessed. In both cultures, the gene expression was quantified after the conditioning of 24 hours in HLCs exposed to 30 mM APAP for 8 hours. The gene expression of 3D injured HLCs are shown in Figure 6 relative to 2D injured HLCs.

The results showed that 3D-cultured HLCs had lower expression of necroptotic, apoptotic and ER stress genes, i.e., *RIPK3* (p < 0.01), *BAX* and *ATF-6* (p < 0.001), respectively, than 2D-cultured HLCs. Conversely, *TNF-A* was more up-regulated in 3D cultures (p < 0.001). These differences might have been related with the gradients of nutrients, oxygen and, consequently, APAP, generated within the spheroids, not exposing all cells to the same drug concentration as in 2D-cultured HLCs. Moreover, 3D-cultured HLCs might have displayed a higher hepatoprotective potential than 2D-cultured. Likewise, it was previously suggested that 3D cultures might had a higher ability to scavenge reactive species comparing to 2D models.[38] Therefore, further studies should focus on the APAP-induced mechanisms in 3D-cultured HLCs. Due to time limitations, APAP-induced injury and the effect of MSC secretome was continued only in 2D-cultured HLCs.

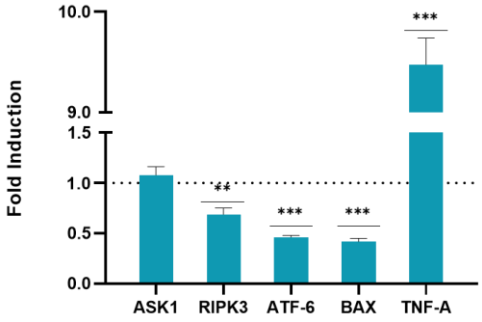

Figure 6 - 3D-cultured HLCs inhibited APAP-related pathways. Gene expression of 3D-cultured HLCs is presented relative to 2D-cultures HLCs both exposed to 30 mM APAP for 8 hours and recovered at the end of the conditioning period. Data represented as average ± SD (n=1-3). **, *** significantly differs from 2D and 3D-cultured HLCs with p < 0.01 and p < 0.001, respectively.

Priming with the SOS medium exerted pro-angiogenic and regenerative effects in hnUCM-MSCs

The capacity that MSCs have to answer accordingly to their surrounding microenvironment, enabled their pre-conditioning with pro-inflammatory cytokines or injured liver tissue, which resembled the *in vivo* environment, enhancing the secretion of paracrine factors.[22,20,48] Considering that APAP treatment might have induced the HLCs' secretion of pro-inflammatory cytokines into their medium (SOS medium), as suggested by the induction of ER stress and apoptosis pathways in HLCs upon APAP exposure, the incubation of hnUCM-MSCs with the SOS medium might modulate them into a more anti-inflammatory and/or pro-regenerative phenotype.

Thus, the next step was to evaluate the effect of priming hnUCM-MSCs with the SOS medium (pMSC-CM) for 24 hours in serum-free conditions. After priming, the medium was replaced by fresh α-MEM without FBS and pMSC-CM was collected 48 hours after. hnUCM-MSCs not exposed to the SOS medium were used as control (cMSC-CM). As a normalization step to ensure that hnUCM-MSCs were always exposed to the same SOS medium conditions, the total protein of HLCs after an 8-hour exposure to 30 mM APAP followed by the 24-hour conditioning period, from which the SOS medium was produced, was quantified (data not shown) and the ratio of total protein per cm^2 was maintained.

The morphological changes of hnUCM-MSCs during this process are presented in Figure 7. 2 days post-inoculation with 5 % (v/v) FBS (Figure 7 a)), hnUCM-MSCs presented the expected 60 % confluence and fibroblast-like morphology. At day 5 post-inoculation, 72 hours after priming with the SOS medium 5x concentrated (Figure 7 b)), the primed hnUCM-MSCs displayed higher confluency when compared to the non-primed hnUCM-MSCs (Figure

7 c)), as also confirmed by total protein quantification (data not shown) suggesting that the inflammatory signals in the SOS medium might have triggered a proliferative response in hnUCM-MSCs.

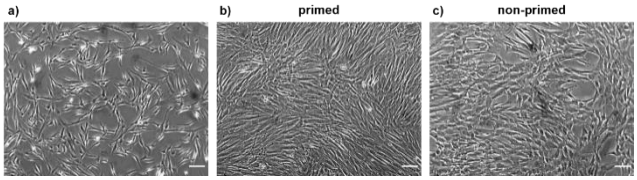

Figure 7 - Priming with the SOS medium increased hnUCM-MSCs' confluency. a) hnUCM-MSCs' morphology 2 days post-inoculation; b) hnUCM-MSCs' morphology 5 days post-inoculation and 72 hours after the priming with the SOS medium; c) non-primed hnUCM-MSCs' morphology 5 days post-inoculation. Scale bar = 100 µm.

The gene expression profile of the primed hnUCM-MSCs was evaluated and compared to that of non-primed hnUCM-MSCs. From all the known growth factors and cytokines secreted by MSCs, we assessed the expression of key genes (Figure 8) either involved in hepatocyte proliferation and regeneration (*IL-6* and *TNF-A*) or with anti-fibrotic (*HGF*), chemoattractive (*SDF-1*) and pro-angiogenic (*VEGF-A* and *SDF-1*) properties.

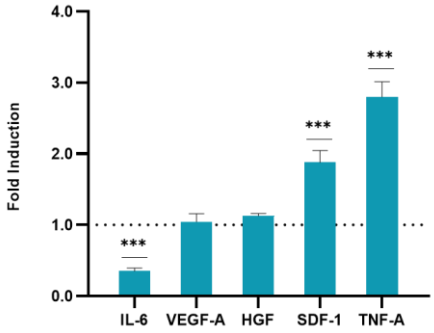

Figure 8 - Enhanced pro-angiogenic effects in hnUCM-MSCs primed with the SOS medium. Gene expression of hnUCM-MSCs primed for 24 hours with the SOS medium following a 48-hour incubation with fresh medium is presented relative to non-primed hnUCM-MSCs. Data represented as average ± SD (n=2-3). *** significantly differs from the non-primed hnUCM-MSCs gene expression with $p < 0.001$

As seen in Figure 8, *SDF-1* and *TNF-A* ($p < 0.001$) showed a significant up-regulation in primed hnUCM-MSCs comparatively to non-primed hnUCM-MSCs.

SDF-1 has been identified in MSCs amniotic fluid stem cells CM, along with VEGF. These two cytokines have been described to act synergically in mediating angiogenesis.[49] Moreover, SDF-1 has been identified in UC-MSCs CM and its chemoattractive activity induced the recruitment of cells in injured tissue, enhancing the proliferation and exerting therapeutical relevance.[50] Therefore, the *SDF-1* high expression values in primed hnUCM-MSCs showed that its pro-angiogenic effect was activated. Additionally, TNF-α has revealed to be pro-angiogenic and cytoprotective.[51] The great expression of *TNF-A* in primed hnUCM-MSCs might be beneficial for the initiation of liver regeneration.

IL-6 is a multifunctional cytokine that mediates cell proliferation, differentiation, survival and apoptosis via the JAK-signal transducer and activator of transcription (STAT) pathway, the MAPK pathway and the PI3K/Akt pathway.[52] IL-6 has a dual role as a pro-inflammatory cytokine[53] and as a hepatoprotective factor, exerting pro-regenerative[54] and anti-apoptotic effects[55] through the suppression of NK T cells in the liver.[56] Indeed, IL-6 expressed in MSC-CM had anti-apoptotic effects.[57] Additionally, IL-6 was essential for the proliferation and immunosuppression capacities of MSCs.[58] Moreover, in the hepatocyte cell cycle, TNF-α and IL-6 are known to initiate the liver regeneration cycle.[59] Therefore, IL-6 presence in the MSC-CM might stimulate hepatocyte proliferation and regeneration. However, our results showed *IL-6* inhibition ($p < 0.001$) in primed hnUCM-MSCs. This lower gene expression relatively to control might have been related with the inflammatory signals present in the SOS medium, for instance *ATF-6*, modulating MSCs into a more anti-inflammatory phenotype and suppressing *IL-6* due to its pro-inflammatory role.

MSCs are known to secrete HGF and VEGF-α in high quantities. VEGF-α has an important role in cell protection and survival, being known to induce angiogenesis and HGF is an important anti-fibrotic cytokine known to induce MSCs differentiation into hepatocytes *in vitro*.[60] HGF is recognised by the c-Met receptor in hepatocytes which triggers the activation of a tyrosine kinase signalling cascade, resulting in the stimulation of cell proliferation and in the induction of HSCs apoptosis (anti-fibrotic effect). Indeed, MSCs-CM with high levels of HGF inhibited the activation of HSCs *in vitro*.[22] Moreover, MSCs overexpressing HGF resulted in reduced liver failure and mortality in rats but also improved the functionality of hepatocytes.[61] Furthermore, the secretion of VEGF-α and HGF significantly increased in stress-induced environments, namely in cultures with TNF-α, LPS or hypoxia stimulus.[62] However, in this work, the priming did not enhance the secretion of neither *VEGF-α* or *HGF*, since their expression values were similar to control. This result might suggest that the inflammatory signals presented in the SOS medium were not enough to enhance the expression of these genes, probably related with the intrinsic regeneration of HLCs seen when the SOS medium was harvested.

Overall, the expression values of the assessed genes concluded that upon priming with the SOS medium, hnUCM-MSCs were modulated into a more anti-inflammatory phenotype, with pro-angiogenic effect. The pMSC-CM might exert hepatic pro-regenerative effects due to the presence of these soluble mediators, enhancing the formation of new microvasculature from pre-existing blood vessels and priming the hepatocytes cell cycle. Therefore, to assess whether the priming exerts the above-mentioned effects we evaluated the pMSC-CM effect on HLCs.

Evaluation of the regenerative effect of primed MSC secretome in APAP-induced liver injury *in vitro* model

Inducing liver injury through APAP exposure

The MSC secretome has improved several diseases outcomes through the counterplay between the secreted trophic factors and cells. Bearing in mind the objective of this work, the potential effects of the pMSC-CM secretome in promoting the regeneration in an APAP-induced HLC *in vitro* model were herein assessed *in vitro*. HLCs were injured at D27 with 30 mM APAP for 24 hours, maintaining the same time of exposure as the established in the APAP dose-response curve. Afterwards, the cells were incubated either with cMSC-CM or pMSC-CM 10x concentrated, for other 24 hours. To evaluate the hepatic injury in HLCs exposed to 30 mM APAP for 24 hours (prior to treatment with MSC-CM), we analysed the panel of genes involved in APAP-induced hepatotoxicity. Results are shown in Figure 9 relative to non-injured HLCs recovered at D28.

The results presented in Figure 9 showed than *ASK1* ($p < 0.05$), *ATF-6* and *TNF-A* ($p < 0.001$) were significantly overexpressed relatively to non-injured cells, indicating the APAP-induced hepatotoxicity, as expected, namely, the mitochondrial and ER stress. Moreover, the *HNF4-A* ($p < 0.001$) is dramatically reduced, relatively to control, indicating the existence of hepatic injury. After inducing the injury, we must evaluate the regenerative effect of pMSC-CM in injured HLCs.

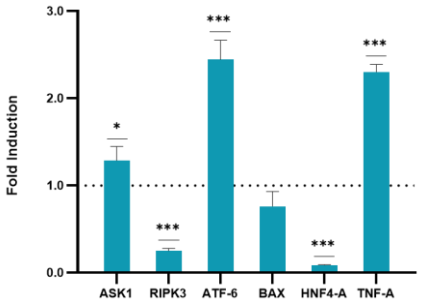

Figure 9 - Mitochondrial and oxidative stress were induced in HLCs following APAP exposure. Gene expression of HLCs exposed to 30 mM APAP for 24 hours is presented relative to non-injured HLCs recovered at D28. Data represented as average ± SD (n=1-3). *, *** significantly differs from the non-injured HLCs gene expression with $p < 0.05$ and $p < 0.001$, respectively.

pMSC-CM displayed a regenerative effect in APAP-induced injury in vitro model

To evaluate the MSC secretome (MSC-CM) effect on the HLCs regeneration after APAP-induced injury, we analysed the expression of key genes involved in hepatocyte proliferation (*C-MET* and *CCND1*) and angiogenesis (*FGF-2* and *VEGF-A*). Additionally, to assess the effect of the MSC secretome in apoptotic pathways, *BAX* expression was analysed. Gene expression of HLCs exposed to 30 mM APAP for 24 hours and incubated with the primed MSC secretome (pMSC-CM) or the control MSC secretome (cMSC-CM) for other 24 hours is presented in Figure 10. Results are presented relative to HLCs injured with 30 mM APAP for 24 hours and incubated with their basal medium for other 24 hours (control).

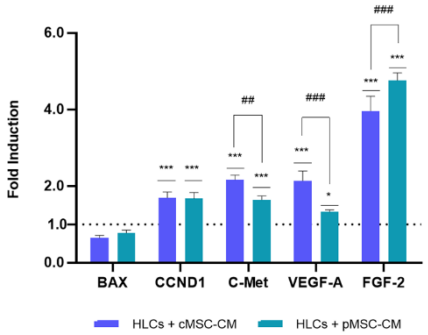

Figure 10 - Regenerative genes were up-regulated in HLCs exposed to the MSC secretome. Gene expression of HLCs with cMSC-CM and pMSC-CM 10x concentrated, after a 24-hour exposure to 30 mM APAP, is presented relative to HLCs exposed to 30 mM APAP for 24 hours incubated with their basal medium (control) for other 24 hours. Data represented as average ± SD (n=2-3). *, *** significantly differs from the control gene expression with $p < 0.05$ and $p < 0.001$, respectively. ##, ### significative difference between injured HLCs with cMSC-CM and with pMSC-CM with $p < 0.01$ and $p < 0.001$, respectively.

The genes involved in the hepatic regeneration, proliferation and angiogenesis – *CCND1*, *C-MET*, *VEGF-α* and *FGF-2* – were overexpressed ($p < 0.05$) in both MSC secretome conditions when compared to control. Nevertheless, the expression level of *BAX* was maintained, indicating that both primed and non-primed MSC secretome did not influence apoptosis.

The priming phase of liver regeneration is mediated by TNF-α and IL-6, which induce the transcription of cyclin D1, for instance. Even though *CCND1* (gene for cyclin D1) expression increased upon treatment with both MSC-CM conditions relatively to control, the results showed no significant differences between *CCND1* expression in HLCs exposed to pMSC-CM and cMSC-CM. This seemed to suggest that the higher overexpression of *TNF-A* in primed MSCs (Figure 8) did not enhance the *CCND1* expression.

Under inflammatory status, the regenerative genes induce the release of HGF and, consequently, the activation of its hepatocyte receptor c-Met. This receptor plays a crucial role in liver regeneration, activating CDKs and enhancing cell proliferation and survival. Since MSCs expressed *HGF* (Figure 8), the higher available quantity of HGF predictably induced the up-regulation of *C-MET*, relatively to control, in HLCs exposed to the MSC secretome.

Within the pro-regenerative signalling pathways, VEGF-α and FGF-2 are responsible for angiogenesis and duplication of hepatic endothelial cells in the injured liver. These cytokines are crucial to restore the vessel wall (endothelial cells, smooth muscle cells and fibroblast cells) of the liver.[10] Thus, the significant overexpression of *VEGF-A* and *FGF-2* in injured HLCs exposed to the MSC secretome, relatively to control, may suggest that the hepatocyte regeneration was enhanced. This result is concordant with the observed in Du, Z. *et al.* (2013) in which *VEGF-A* higher expression was associated with hepatocyte proliferation after MSC-CM therapy.[63]

The MSC secretome seemed to be beneficial on injured HLCs by enhancing their regenerative pathways. However, the gene expression of HLCs exposed to 30 mM APAP for 24 hours did not evidence clearly which CM condition (cMSC-CM or pMSC-CM) improved the hepatic regeneration to a greater extent, since *VEGF-A* and *C-MET* were more induced in HLCs exposed to cMSC-CM ($p < 0.01$) while *FGF-2* ($p < 0.001$) had a higher induction in HLCs treated with pMSC-CM. This might be related with the level of injury, which corresponded to the APAP IC_{50}, being too high and in this case the CM cannot exert more notorious therapeutic effects.

Given these results, we hypothesized that the MSC secretome therapeutical action could be enhanced under lower APAP concentrations. Thus, in an attempt to distinguish the benefits of the two MSC secretome conditions, we tested their proliferative effect under lower levels of HLC injury. The APAP concentrations herein analysed consisted of the concentration used until this point, the IC_{50} (30 mM); an intermediate (15 mM) and a lower concentration (5 mM); and a control with HLCs not exposed to APAP (0 mM) tested upon a 24-hour incubation. After inducing the injury, the medium was replaced by fresh medium with either pMSC-CM or cMSC-CM 10x concentrated, exposing the cells for 24 hours to the MSC secretome. Finally, the cell viability was measured (Figure 11). The results are presented as a normalization to the positive control (HLCs not exposed to APAP).

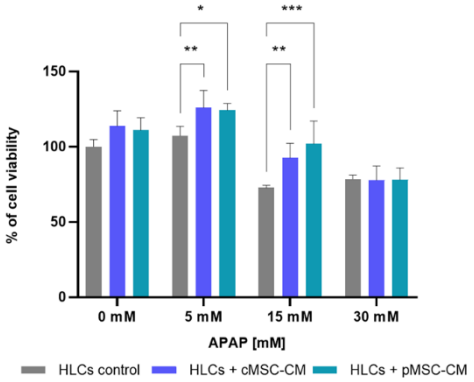

Figure 11 - MSC secretome enhanced HLCs proliferation in lower APAP concentrations. Cell viability of HLCs exposed to different APAP concentrations for 24 hours and incubated with cMSC-CM or pMSC-CM, 10x concentrated, or with their basal medium, for 24 hours. Cell viability percentage was normalized to the positive control (HLCs not exposed to APAP). Data represented as average ± SD (n=1). *, **, *** significantly differs from the injured HLCs with IMDM, cMSC-CM or pMSC-CM gene expression with $p < 0.05$, $p < 0.01$ and $p < 0.001$, respectively.

The results show that the MSC secretome was not toxic for HLCs. Indeed, in HLCs exposed to 5 mM and 15 mM APAP, both cMSC-CM and pMSC-CM, revealed to be beneficial in comparison to not treated HLCs, showing higher cell viability

percentages ($p < 0.05$). However, non-injured HLCs (0 mM APAP) and HLCs exposed to 30 mM APAP, incubated with either cMSC-CM or pMSC-CM did not display significative cell viability alterations. This result seemed to indicate that until a certain concentration of APAP and, consequently, a certain degree of APAP-induced injury, the therapeutic effect of both primed and non-primed MSC secretomes is stimulated. Therefore, the MSC secretome therapeutical action appeared to be between 5 and 15 mM APAP.

Notably, the cell viability percentages presented in Figure 11 did not correspond to the estimated by the APAP dose-response curve (Figure 1). The cell viability in HLCs exposed to 30 mM APAP was superior to the calculated IC_{50}. This result was concordant with the cell morphology seen 24 hours after removing APAP in Figure 2 c), reinforcing the hypothesis that HLCs were able to recover until a certain extension of injury even with their basal medium.

Regarding the priming strategy, in intermediate injuries (15 mM APAP), the pMSC-CM exerted more beneficial effects than cMSC-CM, suggesting that the secreted pro-angiogenic and pro-regenerative factors (Figure 8) seemed to enhance the cell proliferation. Conversely, in a lesser extent of injury (5 mM APAP) the priming did not seem crucial for HLCs regeneration, since cMSC-CM revealed a higher enhancement in cell proliferation.

Concordantly with the up-regulation of regenerative genes in HLCs exposed to the MSC secretome (Figure 10), this CM therapy appeared to be beneficial and enhance the regeneration of APAP-injured HLCs. Particularly, the priming strategy herein applied to hnUCM-MSCs seemed to indicate that in an intermediate APAP concentration (15 mM) the hepatic regeneration was potentiated, appearing to be a favourable liver regenerative therapy.

4. Conclusions and future perspectives

To develop efficient therapies for APAP-induced liver injury, the underlying mechanisms of hepatotoxicity and liver regeneration need to be thoroughly understood. In particular, MSC paracrine activity, which can be modulated according to the surrounding microenvironment, has been demonstrated to present important immunomodulatory and anti-inflammatory effects, representing an interesting therapeutic approach.

Firstly, injury was induced by exposing HLCs to APAP IC_{50} (30 mM) in 2D and 3D cultures. In 2D cultures, it was observed that mitochondrial and ER stress and apoptosis were activated. In contrast, 3D-cultured HLCs had lower expression of necroptotic, apoptotic and ER stress genes and increased upregulation of *TNF-A* when compared to 2D cultures. These differences might be related with gradients of APAP generated within the spheroids and possible hepatoprotective effects previously described in 3D cultures. As such, further studies should focus on the APAP-induced toxicity mechanisms in 3D-cultured HLCs. Nevertheless, given the resultant hepatotoxicity upon APAP incubation, 2D-cultured HLCs were used to evaluate MSC secretome therapeutic effect. Accordingly, the resultant medium from APAP-injured HLCs with inflammatory signals (SOS medium) was then used to prime MSC-derived secretome (pMSC-CM) into a more regenerative phenotype. It was observed that MSCs exposed to SOS medium presented a more anti-inflammatory phenotype, activating pro-angiogenic pathways.

The next step was to evaluate the effect of the MSC secretome in APAP-injured HLCs. Overall, both pMSC-CM and non-primed MSC-CM (cMSC-CM) induced regeneration, proliferation and angiogenic pathways in HLCs. In particular, pMSC-CM induced higher *FGF-2* overexpression than cMSC-CM, which is related to angiogenesis. On the other hand, cMSC-CM induced higher overexpression of *C-MET* and *VEGF-A*, related to cell proliferation and angiogenesis, respectively. As both secretomes exerted beneficial effects on HLCs injured with 30 mM of APAP, lower levels of injury were studied to assess if differential effects could be observed in cell viability. In fact, in an intermediate level of injury (15 mM), pMSC-CM induced higher HLC proliferation while cMSC-CM stimulated higher cell proliferation in a lower injury level (5 mM). Therefore, our results suggest that at lower levels of injury, MSC secretome does not need to be modulated to produce effects at the cell proliferation level but MSC priming strategy seemed to be best suited for intermediate levels of HLC injury.

As differences in cell proliferation upon MSC secretome treatment were observed with different levels of HLC injury, future work should include a broader characterization of HLCs and MSC secretome. Specifically, HLCs should be analysed regarding gene expression, secreted factors and mitochondrial and ER functionality. Moreover, the specific paracrine mediators present in the SOS medium, in the pMSC-CM and in the cMSC-CM should also be determined, through e.g. proteomic analysis.

Furthermore, our results suggested that HLCs were able to activate intrinsic regenerative mechanisms in the 24 hours of conditioning for the production of the SOS medium. Therefore, to increase the presence of inflammatory signals in the SOS medium, we might consider the reduction of the conditioning time.

In the present work, we tested CM 10x concentrated, corresponding to 10 % of the final volume, since it was previously established in our group as an optimized concentration. However, Poll, D. et al. (2008), noticed that low concentrations of MSC-CM in the culture medium revealed a direct anti-apoptotic effect on hepatocytes. Actually, 2% MSC-CM in the culture medium revealed to have better results than 8 %.[43] Thus, it might be interesting to assess the regenerative effect of different CM concentrations in the HLCs regeneration in future work.

In conclusion, this work demonstrated that the medium obtained from an APAP-induced liver injury *in vitro* model (SOS medium) was capable of mimicking the liver injury microenvironment and successfully modulated hnUCM-MSCs into a pro-regenerative phenotype. Therefore, the primed MSC secretome revealed to enhance the hepatic regeneration in intermediate degrees of APAP-induced injury. Although further studies are needed to better understand the regenerative mechanisms potentiated by the primed MSC secretome and in which conditions it is best applied as a hepatic therapy, the work herein achieved showcased the first steps towards establishing a stem cell free-based therapy for hepatic regeneration.

Acknowledgements

This document was written and made publicly available as an institutional academic requirement and as a part of the evaluation of the MSc thesis in Biological Engineering of Daniela Sofia Nunes Ribeiro at Instituto Superior Técnico. The work described herein was performed at the Research Institute of Medicines (iMed.Ulisboa), Faculdade de Farmácia, University of Lisbon (Lisbon, Portugal), during the period April-October 2021, under the supervision of Prof. Joana Paiva Miranda. The thesis was co-supervised at Instituto Superior Técnico by Prof. Cláudia Lobato da Silva.

5. References

1. Suk, K. T. & Kim, D. J. Drug-induced liver injury: present and future. *Clin. Mol. Hepatol.* **18**, 249 (2012).
2. Lee, W. M. Acetaminophen (APAP) hepatotoxicity—Isn't it time for APAP to go away? *J. Hepatol.* **67**, 1324–1331 (2017).
3. Bunchorntavakul, C. & Reddy, K. R. Acetaminophen (APAP or N-Acetyl-p-Aminophenol) and Acute Liver Failure. *Clin. Liver Dis.* **22**, 325–346 (2018).

4. Mazaleuskaya, L. L. *et al.* PharmGKB summary: pathways of acetaminophen metabolism at the therapeutic versus toxic doses. *Pharmacogenet. Genomics* **25**, 416–26 (2015).
5. Ramachandran, A. & Jaeschke, H. Acetaminophen Toxicity: Novel Insights Into Mechanisms and Future Perspectives. *Gene Expr.* **18**, 19–30 (2018).
6. Yan, M., Huo, Y., Yin, S. & Hu, H. Mechanisms of acetaminophen-induced liver injury and its implications for therapeutic interventions. *Redox Biol.* **17**, 274–283 (2018).
7. Liu, X. & Green, R. M. Endoplasmic reticulum stress and liver diseases. *Liver Res.* **3**, 55–64 (2019).
8. Bangru, S. & Kalsotra, A. Cellular and molecular basis of liver regeneration. *Semin. Cell Dev. Biol.* **100**, 74–87 (2020).
9. Gilgenkrantz, H. & Collin de l'Hortet, A. Understanding Liver Regeneration: From Mechanisms to Regenerative Medicine. *Am. J. Pathol.* **188**, 1316–1327 (2018).
10. Abu Rmilah, A. *et al.* Understanding the marvels behind liver regeneration. *WIREs Dev. Biol.* **8**, 1–46 (2019).
11. Apte, U., Limaye, P. B. & Michalopoulos, G. K. Extracellular Signals Involved in Liver Regeneration. in *Liver Regeneration* 65–75 (Elsevier, 2015). doi:10.1016/B978-0-12-420128-6.00005-1.
12. Kaur, S. & Anita, K. Angiogenesis in liver regeneration and fibrosis: "a double-edged sword". *Hepatol. Int.* **7**, 959–968 (2013).
13. Huck, I., Gunewardena, S., Espanol-Suner, R., Willenbring, H. & Apte, U. Hepatocyte Nuclear Factor 4 Alpha Activation Is Essential for Termination of Liver Regeneration in Mice. *Hepatology* **70**, 666–681 (2019).
14. Asrani, S. K., Devarbhavi, H., Eaton, J. & Kamath, P. S. Burden of liver diseases in the world. *J. Hepatol.* **70**, 151–171 (2019).
15. Watanabe, Y., Tsuchiya, A. & Terai, S. The development of mesenchymal stem cell therapy in the present, and the perspective of cell-free therapy in the future. *Clin. Mol. Hepatol.* **27**, 70–80 (2021).
16. L., P. K. *et al.* The mesenchymal stem cell secretome: A new paradigm towards cell-free therapeutic mode in regenerative medicine. *Cytokine Growth Factor Rev.* **46**, 1–9 (2019).
17. Duncan, A. W., Dorrell, C. & Grompe, M. Stem Cells and Liver Regeneration. *Gastroenterology* **137**, 466–481 (2009).
18. Boyd, A., Newsome, P. & Lu, W.-Y. The role of stem cells in liver injury and repair. *Expert Rev. Gastroenterol. Hepatol.* **13**, 623–631 (2019).
19. Zhang, Y., Li, Y., Zhang, L., Li, J. & Zhu, C. Mesenchymal stem cells: potential application for the treatment of hepatic cirrhosis. *Stem Cell Res. Ther.* **9**, 59 (2018).
20. Waterman, R. S., Tomchuck, S. L., Henkle, S. L. & Betancourt, A. M. A New Mesenchymal Stem Cell (MSC) Paradigm: Polarization into a Pro-Inflammatory MSC1 or an Immunosuppressive MSC2 Phenotype. *PLoS One* **5**, e10088 (2010).
21. Haque, N., Rahman, M. T., Abu Kasim, N. H. & Alabsi, A. M. Hypoxic Culture Conditions as a Solution for Mesenchymal Stem Cell Based Regenerative Therapy. *Sci. World J.* **2013**, 1–12 (2013).
22. Choi, J. S., Ryu, H. A., Cheon, S. H. & Kim, S. W. Human Adipose Derived Stem Cells Exhibit Enhanced Liver Regeneration in Acute Liver Injury by Controlled Releasing Hepatocyte Growth Factor. *Cell. Physiol. Biochem.* **52**, 935–950 (2019).
23. Oyagi, S. *et al.* Therapeutic effect of transplanting HGF-treated bone marrow mesenchymal cells into CCl4-injured rats. *J. Hepatol.* **44**, 742–748 (2006).
24. Zimmermann, J. & McDevitt, T. C. Engineering the 3D MSC Spheroid Microenvironment to Enhance Immunomodulation. *Cytotherapy* **20**, S106 (2018).
25. Zhang, X., Hu, M.-G., Pan, K., Li, C.-H. & Liu, R. 3D Spheroid Culture Enhances the Expression of Antifibrotic Factors in Human Adipose-Derived MSCs and Improves Their Therapeutic Effects on Hepatic Fibrosis. *Stem Cells Int.* **2016**, 1–8 (2016).
26. Lee, B.-C. & Kang, K.-S. Functional enhancement strategies for immunomodulation of mesenchymal stem cells and their therapeutic application. *Stem Cell Res. Ther.* **11**, 397 (2020).
27. Ma, H.-C., Shi, X.-L., Ren, H.-Z., Yuan, X.-W. & Ding, Y.-T. Targeted migration of mesenchymal stem cells modified with CXCR4 to acute failing liver improves liver regeneration. *World J. Gastroenterol.* **20**, 14884 (2014).
28. Miranda, J. P. *et al.* The Human Umbilical Cord Tissue-Derived MSC Population UCX ® Promotes Early Motogenic Effects on Keratinocytes and Fibroblasts and G-CSF-Mediated Mobilization of BM-MSCs when Transplanted In Vivo. *Cell Transplant.* **24**, 865–877 (2015).
29. Santos, J. M. *et al.* Three-dimensional spheroid cell culture of umbilical cord tissue-derived mesenchymal stromal cells leads to enhanced paracrine induction of wound healing. *Stem Cell Res. Ther.* **6**, 90 (2015).
30. Rajan, N., Habermehl, J., Coté, M.-F., Doillon, C. J. & Mantovani, D. Preparation of ready-to-use, storable and reconstituted type I collagen from rat tail tendon for tissue engineering applications. *Nat. Protoc.* **1**, 2753–2758 (2006).
31. Cipriano, M. *et al.* The role of epigenetic modifiers in extended cultures of functional hepatocyte-like cells derived from human neonatal mesenchymal stem cells. *Arch. Toxicol.* **91**, 2469–2489 (2017).
32. Cipriano, M. *et al.* Self-assembled 3D spheroids and hollow-fibre bioreactors improve MSC-derived hepatocyte-like cell maturation in vitro. *Arch. Toxicol.* **91**, 1815–1832 (2017).
33. Liu, Y. *et al.* Animal models of chronic liver diseases. *Am. J. Physiol. Liver Physiol.* **304**, G449–G468 (2013).
34. Serras, A. S. *et al.* A Critical Perspective on 3D Liver Models for Drug Metabolism and Toxicology Studies. *Front. Cell Dev. Biol.* **9**, 1–30 (2021).
35. Zeilinger, K., Freyer, N., Damm, G., Seehofer, D. & Knöspel, F. Cell sources for in vitro human liver cell culture models. *Exp. Biol. Med.* **241**, 1684–1698 (2016).
36. Lee, C.-W., Chen, Y.-F., Wu, H.-H. & Lee, O. K. Historical Perspectives and Advances in Mesenchymal Stem Cell Research for the Treatment of Liver Diseases. *Gastroenterology* **154**, 46–56 (2018).
37. Yin, F., Wang, W.-Y. & Jiang, W.-H. Human umbilical cord mesenchymal stem cells ameliorate liver fibrosis in vitro and in vivo : From biological characteristics to therapeutic mechanisms. *World J. Stem Cells* **11**, 548–564 (2019).
38. Cipriano, M. *et al.* Nevirapine Biotransformation Insights: An Integrated In Vitro Approach Unveils the Biocompetence and Glutathiolomic Profile of a Human Hepatocyte-Like Cell 3D Model. *Int. J. Mol. Sci.* **21**, 3998 (2020).
39. Kim, D. E. *et al.* Prediction of drug-induced immune-mediated hepatotoxicity using hepatocyte-like cells derived from human embryonic stem cells. *Toxicology* **387**, 1–9 (2017).
40. Florentino, R. M. *et al.* Cellular Location of HNF4α is Linked With Terminal Liver Failure in Humans. *Hepatol. Commun.* **4**, 859–875 (2020).
41. Nishikawa, T. *et al.* Resetting the transcription factor network reverses terminal chronic hepatic failure. *J. Clin. Invest.* **125**, 1533–1544 (2015).
42. Lazarevich, N. L. *et al.* Progression of HCC in mice is associated with a downregulation in the expression of hepatocyte nuclear factors. *Hepatology* **39**, 1038–1047 (2004).
43. Van Poll, D. *et al.* Mesenchymal stem cell-derived molecules directly modulate hepatocellular death and regeneration in vitro and in vivo. *Hepatology* **47**, 1634–1643 (2008).
44. Parameswaran, N. & Patial, S. Tumor Necrosis Factor-α Signaling in Macrophages. *Crit. Rev. Eukaryot. Gene Expr.* **20**, 87–103 (2010).
45. Pinheiro, P. F. *et al.* Hepatocyte spheroids as a competent in vitro system for drug biotransformation studies: nevirapine as a bioactivation case study. *Arch. Toxicol.* **91**, 1199–1211 (2017).
46. Takayama, K. *et al.* 3D spheroid culture of hESC/hiPSC-derived hepatocyte-like cells for drug toxicity testing. *Biomaterials* **34**, 1781–1789 (2013).
47. Ramasamy, T. S., Yu, J. S. L., Selden, C., Hodgson, H. & Cui, W. Application of Three-Dimensional Culture Conditions to Human Embryonic Stem Cell-Derived Definitive Endoderm Cells Enhances Hepatocyte Differentiation and Functionality. *Tissue Eng. Part A* **19**, 360–367 (2013).
48. Mohsin, S. *et al.* Enhanced hepatic differentiation of mesenchymal stem cells after pretreatment with injured liver tissue. *Differentiation* **81**, 42–48 (2011).
49. Mirabella, T., Cilli, M., Carlone, S., Cancedda, R. & Gentili, C. Amniotic liquid derived stem cells as reservoir of secreted angiogenic factors capable of stimulating neo-arteriogenesis in an ischemic model. *Biomaterials* **32**, 3689–3699 (2011).
50. SHEN, C. *et al.* Conditioned medium from umbilical cord mesenchymal stem cells induces migration and angiogenesis. *Mol. Med. Rep.* **12**, 20–30 (2015).
51. Kelly, M. L. *et al.* TNF receptor 2, not TNF receptor 1, enhances mesenchymal stem cell-mediated cardiac protection following acute ischemia. *Shock* **33**, 602–7 (2010).
52. HEINRICH, P. C. *et al.* Principles of interleukin (IL)-6-type cytokine signalling and its regulation. *Biochem. J.* **374**, 1–20 (2003).
53. Bourdi, M. *et al.* Role of IL-6 in an IL-10 and IL-4 Double Knockout Mouse Model Uniquely Susceptible to Acetaminophen-Induced Liver Injury. *Chem. Res. Toxicol.* **20**, 208–216 (2007).
54. James, L. P., Lamps, L. W., McCullough, S. & Hinson, J. A. Interleukin 6 and hepatocyte regeneration in acetaminophen toxicity in the mouse. *Biochem. Biophys. Res. Commun.* **309**, 857–863 (2003).
55. Kovalovich, K. *et al.* Interleukin-6 Protects against Fas-mediated Death by Establishing a Critical Level of Anti-apoptotic Hepatic Proteins FLIP, Bcl-2, and Bcl-xL. *J. Biol. Chem.* **276**, 26605–26613 (2001).
56. Sun, R., Tian, Z., Kulkarni, S. & Gao, B. IL-6 Prevents T Cell-Mediated Hepatitis via Inhibition of NKT Cells in CD4 + T Cell- and STAT3-Dependent Manners. *J. Immunol.* **172**, 5648–5655 (2004).
57. Hoek, J. B. & Pastorino, J. G. Cellular Signaling Mechanisms in Alcohol-Induced Liver Damage. *Semin. Liver Dis.* **24**, 257–272 (2004).
58. Dorronsoro, A. *et al.* Intracellular role of IL-6 in mesenchymal stromal cell immunosuppression and proliferation. *Sci. Rep.* **10**, 21853 (2020).
59. Fausto, N. & Riehle, K. J. Mechanisms of liver regeneration and their clinical implications. *J. Hepatobiliary. Pancreat. Surg.* **12**, 181–189 (2005).
60. Lai, L. *et al.* Transplantation of MSCs Overexpressing HGF into a Rat Model of Liver Fibrosis. *Mol. Imaging Biol.* **18**, 43–51 (2016).
61. Kim, M. D. *et al.* Therapeutic effect of hepatocyte growth factor-secreting mesenchymal stem cells in a rat model of liver fibrosis. *Exp. Mol. Med.* **46**, e110-10 (2014).
62. Crisostomo, P. R. *et al.* Human mesenchymal stem cells stimulated by TNF-α, LPS, or hypoxia produce growth factors by an NFκB- but not JNK-dependent mechanism. *Am. J. Physiol. Physiol.* **294**, C675–C682 (2008).
63. Du, Z. *et al.* Mesenchymal stem cell–conditioned medium reduces liver injury and enhances regeneration in reduced-size rat liver transplantation. *J. Surg. Res.* **183**, 907–915 (2013).

6. Annexes

Table A - Primers used for qRT-PCR.

Name	Sequence
ASK1_F	CTGCATTTTGGGAAACTCGACT
ASK1_R	AAGGTGGTAAAACAAGGACGG
RIPK3_F	CCAAATCCAGTAACAGGGCG
RIPK3_R	TCTTTAGGGCCTTCTTGCGA
ATF-6_F	GACAGTACCAACGCTTATGCC
ATF-6_R	CTGGCCTTTAGTGGGTGCAG
BAX_F	CCCGAGAGGTCTTTTTCCGAG
BAX_R	CCAGCCCATGATGGTTCTGAT
TNF-A_F	AAGCACACTGGTTTCCACACT
TNF-A_R	TGGGTCCCTGCATATCCGTT
HNF4-A_F	ATTGACAACCTGTTGCAGGA
HNF4-A_R	CGTTGGTTCCCATATGTTCC
IL-6_F	ACTCACCTCTTCAGAACGAATTG
IL-6_R	CCATCTTTGGAAGGTTCAGGTTG
HGF_F	GCTATCGGGGTAAAGACCTACA
HGF_R	CGTAGCGTACCTCTGGATTGC
SDF-1_F	ATTCTCAACACTCCAAACTGTGC
SDF-1_R	ACTTTAGCTTCGGGTCAATGC
VEGF-A_F	AGGGCAGAATCATCACGAAGT
VEGF-A_R	AGGGTCTCGATTGGATGGCA
C-MET_F	AGCAATGGGGAGTGTAAAGAGG
C-MET_R	CCCAGTCTTGTACTCAGCAAC
CCND1_F	GCTGCGAAGTGGAAACCATC
CCND1_R	CCTCCTTCTGCACACATTTGAA
FGF-2_F	AGAAGAGCGACCCTCACATCA
FGF-2_R	CGGTTAGCACACACTCCTTTG